Investigation of the static trim angle effects on the hydrodynamic performances of a semi-planing catamaran in calm water and waves

Aliasghar Moghaddas[1], Hamid Zeraatgar[2*]

[1]PhD candidate, Amirkabir University of Technology, Department of Maritime Engineering, Tehran, Iran

[2 *]Associate professor, Amirkabir University of Technology, Department of Maritime Engineering, Tehran, Iran

[*]Corresponding author (Email: hamidz@aut.ac.ir, Phone: +989123353894)

Abstract

This article uses the model test to investigate the effect of static trim angle on the hydrodynamic performance of a semi-planing catamaran named AUT-SEM00. First, the resistance test results in the calm water at different speeds for static trim angles of 0.00 to 4.00 degrees are presented. The best static trim angle hence the lowest resistance is 2.0º at a speed of 3.78 m/s which leads to the dynamic trim of 2.5º. Then, the model test in three regular waves in a range of static trim angles is conducted, and the results are analyzed. It has been seen that the best static trim angle in comparison to the other rim angle depicts up to 9% less resistance. Additionally, it is shown that the static trim angle does not significantly affect pitch motion and vertical accelerations. As far as the regular wave length is concerned, the pitch and accelerations on CG and FP rapidly increase as wave length increases. There is a strong correlation between vertical acceleration and pitch motion where both have the same tendency concerning the wave length.

Keywords: model test, semi-planing catamaran, static trim angle, calm water, wave.

1. Introduction

Using catamaran is very attractive due to providing a large deck area to carry cargo and passengers. Due to the hydrodynamic lift, the wetted surfaces of semi-planing hulls are reduced, and the reduction of the wetted surfaces also reduces the hulls' resistance. The semi-planing catamaran (SPC) is small in size, about tens to hundreds of tons, and has a maximum Froude Number (Fr) of about 1. Despite lower resistance, the semi-planing vessels compared to displacement ships, have larger acceleration in waves.

Many research studies are conducted on the subject of catamarans. Dansio and Bunt [1] experimentally investigated the wave resistance of a catamaran in calm water in Fr of 0.2 to 0.5. They found that with a reduction of the interference ratio, the distance between two demi-hulls divided by vessel wet length, and waves generated by demi-hulls increase. Millward [2] analyzed the effect of the interference ratio and water depth on catamaran resistance using the analytical-numerical method. He found that the resistance gradually increases as the distance between demi-hulls decreases. Insel and Molland [3] investigated the resistance components

of high-speed catamarans by separating the wave-making and viscous resistance in Fr of 0.2 to 1 and the interference ratio of 0.2 to 0.5. Results showed that the viscous force, despite wave force, is independent of the interference ratio. Also, at high-speeds, the interference of the generated waves is negligible. Zaraphonitis, Spanos, and Papanikolaou [4] conducted an experimental and numerical study on three Wiggly-shaped catamarans in Fr of 0.25 to 0.55 and the interference ratio of 0.2 to 0.4. They concluded that the largest resistance corresponds to the smallest interference ratio. They also found that by changing the demi-hull from symmetric to asymmetric, the resistance decreases due to the reduction of generated wave heights. Fang and Chan [5] investigated seakeeping parameters of high-speed wave-piercing catamarans in oblique waves using two mathematical models. Results showed that wave-piercing catamarans have lower motion in waves than conventional catamarans. Moraes, Vasconcellos, and Latite [6] conducted an analytical study on wave-making resistance for high-speed catamarans having U and V-shape sections in Fr of 0.2 to 0.9 and an interference ratio of 0.2 to 1.0. They found that the U or V-shape sections do not affect its resistance, for the interference ratio larger than 0.6, and the effect of the interference ratio on the wave-making resistance is insignificant. Souto Zamora, Fernandez, et al. [7] conducted a model test on a displacement catamaran model in Fr of 0.1 to 0.55. Results showed that the resistance, trim, and height of the wave generated between demi-hulls increases as the distance between two demi-hulls increases. Dyachkov and Makov [8] conducted a numerical study on a 23-meter high-speed displacement catamaran at Fr of 0.28 and verified the results with a model test on a scale of 1:12. Then, they developed an analytical method for evaluating seakeeping (heave and pitch) of catamarans with stabilizers and also tried to develop this method for analysis in irregular waves. Sahoo, Salas, and Schwetz [9] experimentally investigated the resistance of high-speed catamarans in calm water. They suggested a regression formula for resistance force considering the distance between two demi-hulls. Lee, Lee, and Kin [10] conducted a study on a small catamaran in Fr of 0.2 to 0.9 and an interference ratio of 0.12 to 0.39 using both experimental and numerical methods. The results showed that decreasing the interference ratio increases the trim and sinkage of the catamaran. Souto, Zamora, Fernandez, et al. [11] analyzed the wave pattern of a catamaran. They concluded that the wave height between two demi-hulls, due to the interference ratio, is higher than those out of two demi-hulls. Zaghi, Briglia, and Mascio [12,13] conducted experimental and numerical studies on the effect of the interference ratio on high-speed catamarans in Fr of 0.2 to 0.8 and the interference ratio of 0.17 to 0.3. The results showed that reducing the distance between two demi-hulls increases the trim angle, which means that the center of pressure moves forward and increases the sinkage of the catamaran.

Broglia, Bouscasse, Jacob, et al. [14] investigated the resistance and motion in waves of a high-speed catamaran named DELFT-372 in Fr of 0.1 to 0.8 using model tests. They recorded resistance, trim, and rise-up and investigated the role of nonlinearity on motion in waves. Castiglione, Stern, Bova, et al. [15] conducted a numerical study on the catamaran in the regular waves in Fr of 0.3 to 0.75. The results showed that the maximum heave occurs at the resonance frequency and the maximum pitch occurs at a frequency lower than the resonance frequency. Broglia, Jacob, Zaglui, et al. [16] experimentally investigated the effect of interference ratio on high-speed catamarans in calm water and found that the resistance in the lowest interference ratio is about 30% more than the resistance in the highest interference ratio. Shahraki, Thomas,

and Amin [17] conducted a towing tank test of a multi-piece model of an INCAT wave-piercing catamaran having a range of lengths (volume) in head sea conditions. They concluded that a center bow with a longer length has a greater slamming load and a greater pitch motion. Shahraki, Davis, Shabani, et al. [18] surveyed to reduce the slamming load of a large wave-piercing catamaran using an experimental method. The results showed that as the height of the deck increases, the slamming load decreases, while the motion increases. Additionally, it showed that the maximum bow motion and the maximum slamming load occur at the same non-dimensional encounter frequency. Farkas, Degiuli, and Martis [19] conducted a numerical study on the interaction of resistance components for a 60-series catamaran in Fr of 0.30 to 0.55 and the interference ratio of 0.23 and 0.47. They concluded that in high Fr, the generated waves are of divergent type, while they are transverse type at moderate Fr, and the interference of the transverse waves causes the formation of a wave trough in the stern increasing the resistance, trim and sinkage. Davis, French, and Thomas [20] conducted an experimental study on the slamming of a 2.5 m hydro-elastic wave-piercing catamaran in a random head wave with a short center bow. The results showed that the slamming load on the hull is 25% to 135% of the catamaran's weight. And, the additional bending moment caused by the slamming load is 11% higher than the calm water bending moment. Lavroff, Davis, Holloway, et al. [21] experimentally investigated wave shock loads on wave-piercing catamarans using a multi-piece model. They concluded that slamming energy decreases along the catamaran length by a damping ratio of 0.02 to 0.06 which the damping ratio depends on the internal friction mechanisms of the ship. Fitriadhy, Razali, and Mansor [22] investigated the seakeeping of a round-bilge catamaran in waves using computational fluid dynamics considering Fr, the distance between two demi-hulls ratios, and the wavelength to ship length ratio. The results showed that the heave and pitch motion of a round-bilge catamaran is significantly affected by Fr and the wavelength to ship length ratio. Farkas, Degiuli, and Martic [23] numerically investigated the interference resistance (IF) for a series 60 catamaran. The results show that interference effects are more significant for narrower catamaran configurations and that the minimum of the IF curve shifts towards higher values of Fr. Also, obtained wave elevations are significantly higher for narrower configurations. Fitriadhy, Adam, Amalina, et al. [24] conducted a numerical study on a V-shape high-speed catamaran in Fr of 0.5 and 1.0. Results showed that RAO decreases as wavelength increases for wavelength less than 0.75 meters. And, as the wave height increases, RAO increases, too. Lin, Hsieh, Lu, et al. [25] investigated the seakeeping performance of a wave-piercing catamaran called CAT-I using a numerical method by Star CCM+ software, a RANS method and a potential flow method. It showed that, among the three methods, the RANS results highly coincided with the experimental results. Chen, Song, and Fun [26] investigated the high-order boundary element method (HOBEN) for the evaluation of a high-speed catamaran performance at Fr of 0.1 to 1.0 and the interference ratio of 0.2 to 1.0. Results showed that for Fr higher than 0.5, the waves generated between two demi-hulls are divergent type and the interaction caused by transverse waves is negligible. And, the interaction between the waves in Fr of 0.4 to 0.7 highly affects the resistance, trim, and sinkage. Shabani, Lavroff, Holloway, et al. [27] designed a bow and a wet-deck to reduce motion and loads using a multi-piece model of a wave-piercing catamaran hull. They conducted 200 model tests in head seas equivalent to wave heights of 2.70, 4.00, and 5.40 meters of the full-scale ship. The results showed that increasing the height of the wet-deck increases the

vertical acceleration of the vessel and reduces the slamming load at a certain speed. Also, the slamming load is 18% to 105% of the ship's weight, which depends on the center bow location and the wave height. They found that reducing the speed from 38 knots to 20 knots can reduce 30% of the load caused by the slamming in a regular wave. Hasheminasab, Zeraatgar, Moradi, et al. [28] experimentally studied the water entry of twin wedge sections as the catamaran sections. This study is carried out on a set of twin wedges of 7, 15, and 20-degree deadrise angles. The results show that the effect of the distance between two demi-hulls on the peak pressure is negligible. Also, the pressure on the non-vertical side of an asymmetry wedge is considerably lower than that on the equivalent symmetry wedge. Miao, Zhao, and Wan [29] conducted a numerical optimization study on an S60 catamaran for resistance reduction based on a consideration of the demi-hull shape and separation. Three free-form deformations (FFD)-related parameters and the separation distance of the demi-hulls are selected as four design variables with two geometric constraints imposed. The total resistance for Fr 0.4 and 0.45 are taken as the two objective functions. Results showed that a maximum resistance reduction of 20.52% for OPT1 and 15.00% for OPT2 are achieved by the optimal catamaran designs for Fr 0.4 and 0.45, respectively. Three optimal catamaran designs are selected from the Pareto front for numerical simulations using RANS-based solver naoe-FOAM-SJTU. The hydrodynamics of these catamarans are compared in detail to those of the initial catamaran. The total resistances of the three optimal catamarans are greatly reduced at Fr = 0.4, and the total resistance of OPT1 is increased a little (0.17%) at Fr = 0.45, due to a larger IF value. Julianto, Muttaqie, Adiputra, et al. [30] conducted research using the experimental method on hydrodynamics and structure of a wave-piercing catamaran considering the fluid-structure interactions. They found that keel-shaped fins and titanium and aluminum materials can make the structure of the ship more durable and resistant to waves. Liu, Wang, Zhang, et al. [31] conducted numerical studies of seakeeping behavior for a high-speed catamaran with a stern flap advancing in a long crest head wave. Both model-scale and full-scale simulations have been carried out in sea state 6 using an unsteady Reynolds-averaged Navier-Stokes (URANS) solver. Model-scale simulation results indicate that using a stern flap could reduce the catamaran's total resistance and the effects on heave and pitch motions are obvious in sea state 6. The installation of the stern flap shows a significant effect on the reduction of vertical acceleration amplitudes, especially for reducing the occurrence of slamming impact due to the effective control of the model's trim angle. Full-scale simulations have also been conducted and compared with the model scale results. Results show that the effects of the stern flap on heave and pitch motions are the same for both model-scale and full-scale catamarans.

Honaryar, Ghiasi, and Honaryar [32] investigated a new phenomenon due to interference phenomenon in the dynamic response of catamarans. The results of catamaran dynamic response reveal that not only does its resistance reduce substantially up to 15%, but also trim angle diminishes by 30% as the distance between two demi-hulls decreases in semi-planing and planing modes. Dogrul, Kahramanoglu, and Cakici [33] focused on the numerical investigation of Delft catamaran 372 which is widely used for benchmarking. Unsteady RANS analyses were conducted at Fr 0.3 in regular head wave conditions. The main highlights of this study are the comprehensive validation study with the literature and the calculation of the interference factor (IF) through total and added resistance in waves. Motion and added

resistance transfer functions were obtained for catamaran and demi-hull geometries. It is concluded that the effects of interference factors in waves are highly important in catamaran forms. Allamah, Lavroff, Holloway, et al. [34] conducted a Full-scale CFD simulation to investigate the pressure distributions and resultant global loads acting on the 98 m INCAT wave-piercer catamaran HSV2 Swift at a forward speed of 20 knots, validated against sea trial tests. Splitting forces are found to have a longitudinal distribution along the catamaran hull, which causes prying moments. Peak values for LBM are examined relative to the corresponding instantaneous wave height prior to the slam event. In addition, it is found that pitch acceleration has a linear correlation with LBM slam loads. Iqbal, Budiarto, Hidayat, et al. [35] numerically investigated the use of foil-shaped center bulb in catamaran fishing vessels at Fr 0.15 to Fr 0.35. The results showed that the best model was found in Model 6, where the length of the center bulb was 15% greater while the width and height were smaller by 10% from the original one. Model 6 can reduce resistance by 10.68%.Wang, Zhu, Zha, et al. [36] performed experimental tests and numerical investigation on a planing catamaran under different displacements to analyze the resistance characteristics and mechanism of the tunnel flow. Model tests are conducted in a towing tank for the in Fr of 0.76 to 1.93. Numerical results of pressure, comparisons of wave profile along transom stern centerline, lift distribution on the tunnel, and components of tunnel lift are presented and compared for the analysis of tunnel flow under different displacements. The tunnel could contribute the maximum lift of about 26% of the ship weight in the case of $M = 202.9$ kg. This study would provide a better understanding of hydrodynamics and the aerodynamics of the tunnel for the planing catamaran. Farkas, Degiuli, Tomljenovic, et al. [37] numerically investigated the interference effect for the Delft 372 catamaran. The results of analyzing the wave profile in the longitudinal center plane of the catamaran with the distance between the hulls equal to 0.233, reveal that at a lower Fr a larger wave crest was obtained behind the stern of the ship compared to a wave crest at a higher Fr. Kiryanto, Santosa, Samuel, et al. [38] numerically studied seakeeping performance of a hospital catamaran ship to handle the COVID-19 pandemic in Indonesia. They investigated a catamaran ship performance at two Fr of 0.23 and 0.31. They found that Fr plays a significant role in motion response, enabling the designers of the hospital ship to predict seakeeping behavior with a satisfactory approximation during the very early design stages. Sugianto, Chen, and Permadi [39] numerically studied the effectiveness of waste collection using a monohull and catamaran fitted with a forward conveyor using Open FOAM software. The results show the marine debris flows at two Fr of 0.08 and 0.16 much more conveniently through the conveyor fitted in front of the catamaran model than in the monohull model. In addition, considering the front-side hull flow, the catamaran model is superior since marine debris can approach the ship easily. Sulistyawati, Sudjasta, and Waskito [40] conducted a comparative numerical study of monohull rounded and chine catamarans on the squat factor in shallow water by varying the water depth ratio h/T 1.2, 1.3, and 1.5 at Fr 0.25, 0.50 and 0.75. The analysis is also carried out on the sinkage and trim factors by varying the ship's trim with changes in LCG points and variations in speed. The overall analysis shows that monohull has a remarkable effect on shallow water at $Fr<0.3$. While at higher speeds, catamarans have a lower influence on the squat, sinkage and trim factors in shallow water conditions. Windyandari, Sugeng, Ridwan, et al. [41] Numerically investigated the hexagonal catamaran hull form on the deadrise angle, angle of attack, and stern angle variation at Fr=0.30. Results

showed that the hexagonal catamaran hulls have better seakeeping performance in the beam sea. However, the conventional catamaran has demonstrated superiority over the hexagonal catamaran in the bow quartering and head sea conditions.

Having considered all cited references, the static trim angle effects on the catamaran performances of SPC have not been addressed. The goal of this study is to investigate the hydrodynamic performances of a SPC in calm water and waves using experiments. For this purpose, a SPC model which is called AUT-SEM00 is initially tested in calm water in Fr of 0.13 to 1.02 at static trim angles of 1º, 2º, 3º, and 4º. The best static trim angle corresponding to the lowest resistance at the service speed of the craft equivalent to Fr of 0.83 is determined. Additionally, at Fr of 0.83 and for the same range of static trim angle, motion in regular head waves in wavelength to length between fore and aft perpendiculars of ships (L_{BP}) ratio of 1, 1.5, and 2 are tested. The results of the conducted model tests are analyzed to show the effect of the static trim angle on the hydrodynamic performances of a SPC. The details of the geometry of the catamaran and experiments and the data generated in this study are illustrated which can be also employed for validation of future numerical simulations.

2. A brief review of ship motion principles

A ship is moving in a regular cosine wave defined at CG as follows:

$$\zeta(t) = \bar{\zeta}\cos(\omega_e t) \tag{1}$$

$$\omega_e = \omega_w - kv\cos\mu \tag{2}$$

A ship model's motion in regular waves are presented in non-dimensional form as follows:

$$Non-DimPitch = \frac{\bar{\eta}_\theta}{k\bar{\zeta}} \tag{3}$$

$$Non-DimACC = \frac{\bar{\ddot{\zeta}}_3}{g} \tag{4}$$

3. Experimental set-up

3.1 Specifications of AUT-SEM00

The AUT-SEM00 selected for the analysis is a 37.50 meter in-length crew boat. A model of 2.250 meters in length is manufactured for the model tests. Specifications of the AUT-SEM00 as an SPC in full-scale and model size are described in Table 1. Figure 1 demonstrates the geometry of the craft in the form of bodylines and sheer plan.

Table 2 depicts the AUT-SEM00 model hydrostatic properties in trim conditions.

The model is manufactured of composite material with a combination of epoxy resin and glass fibers, and the master is carved using a CNC machine. For this purpose, two demi-hulls are

manufactured, polished, and painted. And, the two demi-hulls are connected with two rigid steel rods.

3.2 Model test facilities

The model tests have been conducted in the National Iranian Marine Laboratory (NIMALA). NIMALA towing tank is a large, 402 meters in length, and high-speed, 19.0 m/s, tank. In this towing tank, resistance, motion in regular and irregular waves, captive model tests of Planar Motion Mechanism type for maneuvering hydrodynamic coefficients, and propeller-open-water and propeller-behind-hull tests are conducted. Tests are performed at speeds of 0.10 to 19.0 m/s where the permissible speed fluctuation is ±0.005 m/s. The NIMALA towing tank can perform model tests for displacement ships, semi-planing, and planing craft. A 6-segment plate-type wave-maker generates regular and irregular waves of several spectrum types up to 0.50 m wave height. A beach-type wave damper is located at the second end of the towing tank for the fast preparation of the next test. Table 3 depicts the NIMALA towing tank specifications.

3.3 Model setup and test scenarios

The model connected to the carriage is shown in Figure 2. In this setup, the resistance of the model is measured by a 1-component load cell. The heave and pitch motion are calculated by the recorded vertical displacement at the aft and fore of the model. Also, two accelerometers are installed at the LCG and FP of the model to record the vertical acceleration in the wave tests.

Two sets of model tests are performed that is resistance in the calm water and motion in waves. Additionally, a parametric study is conducted on the effect of the longitudinal center of gravity, say static trim angle, on the resistance and motion in waves.

3.3.1 Resistance tests

As far as resistance tests are concerned, following the ITTC recommendations [42], tests are performed in the range of 5% less than the minimum speed to 5% more than the maximum speed of the ship. Table 4 shows the model test scenario in the calm water. Altogether, 45 test runs are performed in the calm water.

3.3.2 Motion in waves

The model test in waves is performed in regular head waves. Wave profile, pitch motion, acceleration at the center of gravity (CG), and acceleration at the fore perpendicular (FP) are recorded. To prepare the model for testing in waves, the pitch radius of gyration (r_z) is set to 0.25LPP. Also, to measure the vertical acceleration of the model, two accelerometers are employed, one on the fore perpendicular and the other one on the longitudinal center of gravity. Figure 3 shows a photo of the model on the moment of inertia table.

ITTC has several recommendations for the model tests of ships in waves as follows: the wavelength should be at least in the range of 0.50 L_{PP} to 2.00 L_{PP} and the ratio of wave height to wavelength must remain constant at about $\frac{1}{50}$ [43]. The model test scenario in waves is

shown in Table 5. All tests in waves are conducted at a speed of 3.78 equal to 30 knots for the ship.

4. Results and discussions

4.1 Resistance in the calm water

Following the test scenario of Table 4, more than 45 runs are performed. The rise-up, dynamic trim, and resistance are recorded. Figure 4 shows a photo of the AUT-SEM00 model in the calm water test at a static trim angle of 0.0^o and speed of 4.41 m/s.

Table 6 shows the model test results in the calm water in a range of static trim angles and speeds. Also, The uncertainty of results are presented according to ITTC recommendation [44].

Figure 5 and Figure 6 show the rise-up and dynamic trim as a function of Fr for a range of static trim angles.

As can be seen in Figure 5, the rise-up has two trends where it reduces from zero to a considerable negative value (sinkage) and then it increases which becomes positive (rise-up). The above trends are repeating for five different static trim angles. This consistency of the rise-up trends states that a similar pressure field generates around the model hull at a given Fr disregarding the static trim. The maximum sinkage is about -7 mm which is considerable compared to the model draught. At Fr greater than about 0.6, a rise-up occurs which rapidly increases as Fr increases. It becomes 12 mm at a static trim angle of 4.0^o which is significant. As far as the static trim angle effects on the rise-up are concerned, it governs the rise-up as much as that at Fr=0.84 the rise-up is -2 mm and +12 mm at static trim angles of 0.0^o and 4.0^o, respectively.

The dynamic trim versus Fr has a similar trend in different static trim angles. At a given Fr, the dynamic trim difference is almost the static trim difference. The dynamic trim is negligible for low Fr, up to 0.30. A rapid increase happens where the highest dynamic trim occurs at Fr 0.56. Then, it rapidly decreases. At Fr=0.84, for all cases of static trim angle, the dynamic trim is larger than the static trim angle up to one degree.

Figure 7 shows the resistance of the model in calm water as a function of Fr for different static trim angles.

Figure 7 shows that at Fr about 0.45, the trend of the resistance curve changes, and a hump is appeared. Referring to Figure 5, it can be seen the highest sinkage occurs at the same Fr. A trend change happens after Fr about 0.45, and the sinkage becomes rise-up at Fr about 0.60. This phenomenon can be due to the hydrodynamic lift, which decreases the wetted surface, and as a result, the trend of the resistance is changed.

As far as the static trim angle is concerned, the low static trim angle triggers low resistance in the first area. However, in the second area, the lowest resistance belongs to static trim angles of 3.0^o and 4.0^o, and the highest is for 0.0^o, at Fr=1.0. The best static trim angle for the AUT-

SEM00 at a speed of 3.74 m/s (Fr=0.84) is 2.0^o which has the lowest resistance. In this condition, the dynamic trim is 2.5^o which is acceptable regarding the crew comfort.

4.2 Motion in waves

The second set of model tests is conducted in regular head waves to record model motion as a function of wave characteristics in a range of static trim angles. According to the test scenario of Table 4, more than 15 runs are performed. The time series of wave profile, pitch motion, and acceleration at CG and FP are recorded.

As samples, Figure 8 presents a time series of wave and Figures 9, 10, and 11 present a time series of pitch, and acceleration at CG and FP at Run # 2.

The regular wave is recorded in the towing tank about 50 m apart from the wave-maker. According to Figure 9, its profile is quite regular and repeats the same wave amplitude in each period.

Considering the time series of pitch motion at Run # 2, as shown in Figure 9, it is almost a regular motion. It oscillates about the dynamic trim angle recorded in the calm water, say 0.3^o. For the considered case, the pitch amplitude is 1.9^o and the period of the oscillation is 0.53 seconds which is the encounter wave period. The same behavior is seen for the pitch motion in the rest of the test runs.

Figures 10 and 11 show the time series of the vertical acceleration at CG and FP at Run # 2. Both accelerations are almost repeating in consecutive periods and their mean values are almost zero.

Figures 10 and 11 are clearly non-sinusoidal where their peaks are very sharp. At CG, the upward acceleration is slightly sharper than downward on their peaks. The oscillation period of accelerations is the encounter period, as expected. The same behavior is seen in the rest of the test runs. The average amplitude of accelerations of the considered case on CG and FP are 5.2 and 8.2 m/s^2, respectively

The model test results in waves for a range of static trim angles are presented in Table 7. The results show that the pitch amplitude and acceleration on CG and FP significantly increase as λ/L increases. Additionally, it is observed that the acceleration on FP is larger than on CG, as expected. As far as the static trim angle effect is concerned, there are considerable differences between results in different static trim angles. However, no clear tendency for both pitch motion and acceleration is detected.

Following Equations (3) and (4), non-dimensional pitch, non-dimensional CG accelerations, and non-dimensional FP accelerations are depicted in Figures 12 to 14.

Figures 12 to 14 show that none of the pitch, CG acceleration, and FP acceleration are in the resonance peak condition, for the considered range of wave length. Additionally, trends of the above three curves are almost the same and are rapidly increasing. Overall, it is seen that the static trim angle interference on pitch and acceleration trends is marginal. It can be seen that

the amplitude of CG acceleration has not reached the gravity acceleration, while the amplitude of FP acceleration is well beyond the gravity acceleration.

5. Conclusions

A study on the hydrodynamic performances of a high-speed SPC using model tests is performed. The focus is on the effects of the static trim angle on the craft performances in calm water and waves. For this purpose, resistance, trim, and rise-up in calm water and pitch motion, and vertical acceleration in regular waves are recorded and analyzed. The followings are concluded from the considered case:

- The resistance of SPC in calm water shows a rapid increase as Fr increases. However, two trends are distinguished. The first trend is for Fr up to 0.42 where the resistance increases with a high slope while the second trend occurs for Fr 0.45 to 1.0 which has a low slope in comparison to the first trend. Additionally, the static trim angle of 2.0^o depicts the lowest resistance at the service speed.

- There are considerable differences between results in different static trim angles, as far as motion in waves is considered. However, no clear tendency for both pitch motion and acceleration are detected, for the studied case. The non-dimensional test results in waves show that as λ/L increases, pitch and vertical acceleration rapidly increase.

By evaluating the effect of static trim angle on the resistance and running attitude of a semi-planing catamaran in calm water and waves, the following issues can be considered for future studies:

- Investigating the effect of weight change and geometry change on the performance of semi-planing catamarans in calm water and waves.

Nomenclature

$\bar{\zeta}$	Wave amplitude
ω_w	Wave frequency
ω_e	Encounter frequency
Fr	Froude number
k	Wave number
V	Speed in m/s
V_k	Speed in knot
μ	Wave direction
$\bar{\eta}_i$	Motion amplitude of the i-th motion
ε_i	The i-th phase-lag
$\bar{\ddot{\xi}}_3$	Average amplitude of vertical acceleration
g	Gravity acceleration
L_{WL}	Waterline length

λ_w	Wane length
L_{OA}	Overall length
B_T	Maximum transom beam
T	Draft
Δ	Displacement
ρ	Water density
λ	Scale factor
P_B	Braking power
L_{CG}	Longitudinal center of gravity
TF	Bow draft
TA	Stern draft
θ_s	Static trim angle
l	Tank length
b	Tank width
H	Tank height
h	Tank depth
V_c	Carriage speed
$L_{PP} or\ L_{BP}$	Length between perpendicular
T	Wave period
H_w	Wave height
R_T	Total resistance
θ_D	Dynamic trim
Z_v	Rise up
η_θ	Pitch motion amplitude
$\eta_{CG\ ACC}$	CG acceleration amplitude
$\eta_{FP\ ACC}$	FP acceleration amplitude
U_p	Resistance uncertainty
U_t	Trim uncertainty
U_r	Rise up uncertainty

Reference

[1] Dancio, AA. and Bunt, E. A. “Wave interference effects on a double-hull ship model. as measured by gravity dynamometer," Int. J. Mech. Sci., **32(8)**, pp. 653– 676, (1990), DOI: 10.1016/0020-7403(90)90008-7.

[2] Millward, A. "The effect of hull separation and restricted water depth on catamaran resistance,” Int. J. Trans. R. Inst. Nav. Archit., **134**, pp. 341-349, (1992).

[3] Insel, M. and Molland, A. F. "An investigation into the resistance components of high-speed displacement catamarans," Int. J. R. Inst. Nav. Archit., **134**, pp. 1-20, (1992).

[4] Zaraphonitis, G. Spanos, D. and Papanikolaou, A. "Numerical and experimental study on the wave resistance of fast displacement asymmetric catamarans," Proc. 2nd Int. euro conference HIPER, **1**, (2001).

[5] Fang, C. and Chan, H. “Investigation of seakeeping characteristics of high-speed catamaran in wave”. Int. J. Marine Science and Technology, **12(1)**, pp. 7-15, (2004), DOI: 10.51400/2709-6998.2215.

[6] Moraes, H. B. Vasconcellos, J.M. and Latite, R.G. "Wave resistance for high-speed catamarans," Int. J. Ocean Eng., **31(17-18)**, pp. 2253-2282, (2004), DOI: 10.1016/j.oceaneng 2004.03.012.

[7] Souto, I.A. Zamora, R. Fernandez, D. et al. "Catamaran wave resistance and central wave cuts for CFD validation", 12th International Congress of the International Maritime Association of the Mediterranean (IMAM) , Maritime Transportation and Exploitation of Ocean and Coastal Resources, **1**, pp. 157-165, (2005), DOI: 10.1201/9781439833728 ch18.

[8] Dyachkov, V. and Makov, J. “seakeeping of a fast displacement catamaran”, Int. J. Transport, **XX(1)**. pp. 14-22, (2005), DOI: 10.1080/16484142.2005.9637990.

[9] Sahoo, P.K. Salas, M. and Schwetz, A. "Practical evaluation of resistance of high-speed catamaran hull forms-Part I," Int. J. Ships Offshore Struct., **2(4)**, pp. 307–324, (2007) DOI: 10.1080/17445300701594237.

[10] Lee, S. H. Lee, Y.G. and Kin, S.H. "On the development of a small catamaran boat", Int. J. Ocean Eng., **34(14-15)**, pp. 2061–2073, (2007), DOI: 10.1016/j.oceaneng.

[11] Souto, I.A. Zamora-Rodríguez, R. Fernandez-Gutiérrez, D. et al. "Analysis of the wave system of a catamaran for CFD validation", Int. J. Exp. Fluids, **42(2)**, pp. 321-332, (2007), DOI: 10.1007/s00348-006-0244-4.

[12] Zaghi, S. Broglia, R. and Di Mascio, A. "Experimental and numerical investigations on fast catamarans interference effects", Int. J. Hydrodyn., **22(110.5)**, pp. 545–549, (2010), DOI: 10.1016/S1001-6058(09)60250-X.

[13] Zaghi, S. Broglia, R. and Di Mascio, A. "Analysis of the interference effects for high-speed catamarans by model tests and numerical simulations", Int. J. Ocean Eng., **38(17-18)**, pp. 2110-2122, (2011), DOI: 10.1016/j.oceaneng 2011.09.037.

[14] Broglia, R. Bouscasse, B. Jacob, B. and et al. “Calm Water and Seakeeping Investigation for a Fast Catamaran”. 11th International Conference on Fast Sea Transportation FAST, (2011).

[15] Castiglione, T. Stern, F. Bova, S. et al. “Numerical investigation of the seakeeping behavior of a catamaran advancing in regular head waves”, Int. J. Ocean Eng., **38**, pp. 1806–1822. DOI: 10.1016/j.oceaneng.2011.09.003, (2011).

[16] Broglia, R. Jacob, B. Zaglui, S. and et al. "Experimental investigation of interference effects for high-speed catamarans", Int. J. Ocean Eng., **76(2014)**, pp. 75-85, (2014), DOI: 10.1016/j.oceaneng 2013.12.003.

[17] Shahraki, J. Thomas, J. and Amin, V. “Center bow design for wave piercing catamarans”, 12th International Conference on Fast Sea Transportations FAST'12, Netherland, (2013), DOI:10.13140/RG.2.1.3840.2406.

[18] Shahraki, J. Davis, M. Shabani, B. et al. “Mitigation of Slamming of Large Wave-Piercing Catamarans”, 30th Symposium on Naval Hydrodynamics, Hobart, Tasmania, Australia, (2014).

[19] Farkas, A. Degiuli, N. and Martić, I. "Numerical investigation into the interaction of resistance components for a series 60 catamaran", Int. J. Ocean Eng., **146(August)**, pp. 151–169, (2017), DOI: 10.1016/j.oceaneng 2017.09.043.

[20] Davis, M.R. French, B.J. and Thomas, G.A. “Wave slam on wave piercing catamarans in random head seas”, Int. J. Ocean Eng., **135**, pp. 84-97, (2017), DOI: 10.1016/j.oceaneng.2017.03.007.

[21] Lavroff, J. Davis, M.R. Holloway, D.S. and et al. “Wave impact loads on wave-piercing catamarans”, Int. J. Ocean Eng., **131**, pp. 263–271, (2017), DOI: 10.1016/j.oceaneng.2016.11.015.

[22] Fitriadhy, A. Razali, N. and Aqilah Mansor, A. “Seakeeping performance of a rounded hull catamaran in waves using CFD approach”, Int. J. Mechanical Engineering and Sciences. **11(2)**, pp. 2601-2614, (2017), DOI: https://doi.org/10.15282/jmes.11.2.2017.4.0238.

[23] Farkas, A. Degiuli, N. and Martic, I. “Numerical assessment of interference resistance for a series 60 catamaran”, The VII International Conference on Computational Methods in Marine Engineering, pp. 1016-1027, CIMNE, (2017), DOI: 10.1016/j.oceaneng.2012.06.008.

[24] Fitriadhy, A. Adam, N. Amalina, N. and et al. “Seakeeping prediction of deep-V high-speed catamaran using computational fluid dynamic approach”, Int. J. SINERGI, **22(3)**,pp. 139-148, (2018), DOI: doi.org/10.22441/sinergi.2018.3.001.

[25] Lin, C.T. Hsieh, C.W. Lu, L. and et al. “Investigation of the Seakeeping Performance of Twin Hull Vessels by Different Computational Methods”, J. Taiwan Society of Naval Architect and Marine Engineering, **37(3)**, pp. 127-136, (2018).

[26] Chen, X. Zhu, R. Chuan Song, Y. and et al. "An investigation on HOBEM in evaluating ship wave of high-speed catamaran ship", J. Hydrodyn., **31(3)**, pp. 531-541, (2019), DOI: 10. DOI: 7/s42241-018-0092-8.

[27] Shabani, B. Lavroff, J. Holloway, DS. and et al.. “Center bow and wet-deck design for motion and load reductions in wave piercing catamarans at medium speed”, Int. J. Ships and Offshore Structures. pp. 1-17, (2019), DOI: 10.1080/17445302.2019.1708043.

[28] Hasheminasab, H. Zeraatgar, H. Moradi, et al. “Experimental study on water entry of twin wedges”, Proceedings of the Institution of Mechanical Engineers, Part M, J. Engineering for the Maritime Environment, (2019), DOI: 10.1177/1475090219889236.

[29] Miao, A. Zhao, M. and Wan, D. ”CFD-based multi-objective optimization of S60 Catamaran considering Demihull shape and separation”, Int. J. Applied Ocean Research, **97**, (2020), DOI: 10.1016/j.apor.2020.102071.

[30] Julianto, R.I. Muttaqie, T. Adiputra, R. and et al. “Hydrodynamic and Structural Investigations of Catamaran Design”, Int. J. Procedia Structural Integrity, **27**, pp. 93-100, (2020), DOI: 10.1016/j.prostr.2020.07.013.

[31] Liu, L. Wang, X. He, R. and et al. “CFD prediction of stern flap effect on Catamaran seakeeping behavior in long crest head wave”, Int. J. Applied Ocean Research, **104**, (2020), DOI: 10.1016/j.apor.2020.102367.

[32] Honaryar, A. Ghiasi, M. Liu, P. and et al. “A new phenomenon in interference effect on catamaran dynamic response”, Int. J. Mechanical Sciences, **190**, (2021), DOI: 10.1016/j.ijmecsci.2020.106041.

[33] Dogrul, A. Kahramanoglu, E. and Cakıcı, F. “Numerical prediction of interference factor in motions and added resistance for Delft catamaran 372”, Int. J. Ocean Eng., **223**, (2021), DOI: 10.1016/j.oceaneng.2021.108687.

[34] Almallah, I. Ali-Lavroff, J. Holloway, D. and et al. “Slam load estimation for high-speed catamarans in irregular head seas by full-scale computational fluid dynamics”, Int. J. Ocean Eng., **234**, (2021), DOI:10.1016/j.oceaneng.2021.109160.

[35] Iqbal, M. Budiarto, U. Hidayat, K.Z. et al. ”The influence of foil-shaped center bulb geometry into catamaran fishing vessels resistance”, IOP Conf. Series: Materials Science and Engineering, **1034**, (2021), DOI:10.1088/1757-899X/1034/1/012030.

[36] Wang, H. Zhu, R. Zha, L. and et al. “Experimental and numerical investigation on the resistance characteristics of a high-speed planing catamaran in calm water”, Int. J. Ocean Eng., **258**, (2022), DOI: 10.1016/j.oceaneng.2022.111837.

[37] Farkas, A. Degiuli, N. Tomljenović, I. and et al. “Numerical investigation of interference effects for the Delft 372 catamaran”, In Sustainable Development and Innovations in Marine Technologies, pp. 67-74, CRC Press, (2022), DOI: 10.1177/14750902231197886.

[38] Kiryanto, K. Santosa, A. Samuel, S. et al. “Sea-keeping analysis of hospital catamarans for handling COVID-19 patients on remote islands with a numerical approach”, Int. J. Advanced and Applied Sciences, **9(8)**, pp. 128-135, (2022), DOI:10.21833/ijaas.2022.08.016.

[39] Sugianto, E. Chen, J.H. and Permadi, N.V.A. “Effect of monohull type and catamaran hull type on ocean waste collection behavior using Open FOAM”, Water 2022, **14**, (2022), DOI:10.3390/ w14172623.

[40] Sulistyawati, W. Sudjasta, B. and Waskito, D.Y. “Comparison of shallow water effect on a monohull and chine catamaran”, IOP Conf. Series: Earth and Environmental, IOP Publishing, (2022), DOI:10.1088/1755-1315/972/1/012046.

[41] Windyandari, A. Sugeng, S. Sulaiman Ridwan, M. et al. “Seakeeping behavior of hexagonal catamaran hull form as an alternative geometry design of flat-side hull vessel”, Int. J. Applied Engineering Science, **21(4)**, pp. 1016-1030, (2023), DOI:10.5937/jaes0-41412.

[42] ITTC, “Recommended Procedures and Guidelines”, Testing and Extrapolation Methods high-speed Marine Vehicles Resistance Test, 7.5-02 -05-01, Revision 01, (2002).

[43] ITTC, “Recommended Procedures and Guidelines”, Seakeeping Experiments, 7.5-02 -07-02.1, Revision 04, (2014).

[44] ITTC, “Recommended Procedures and Guidelines”, General guideline for uncertainty analysis in resistance tests. 7.5-02 -02-02, Revision 02, (2014).

Figures

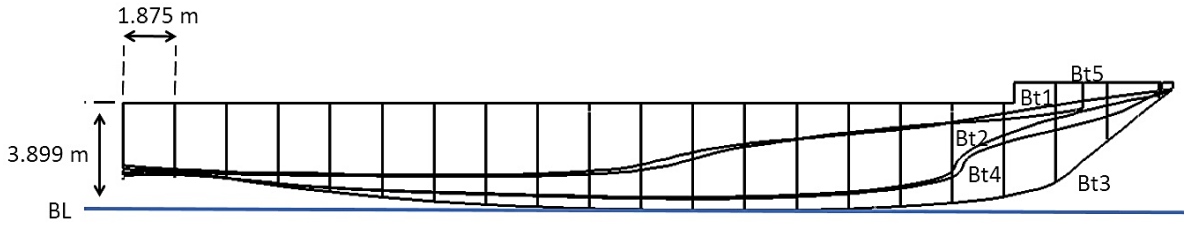

(a) Sheer lines

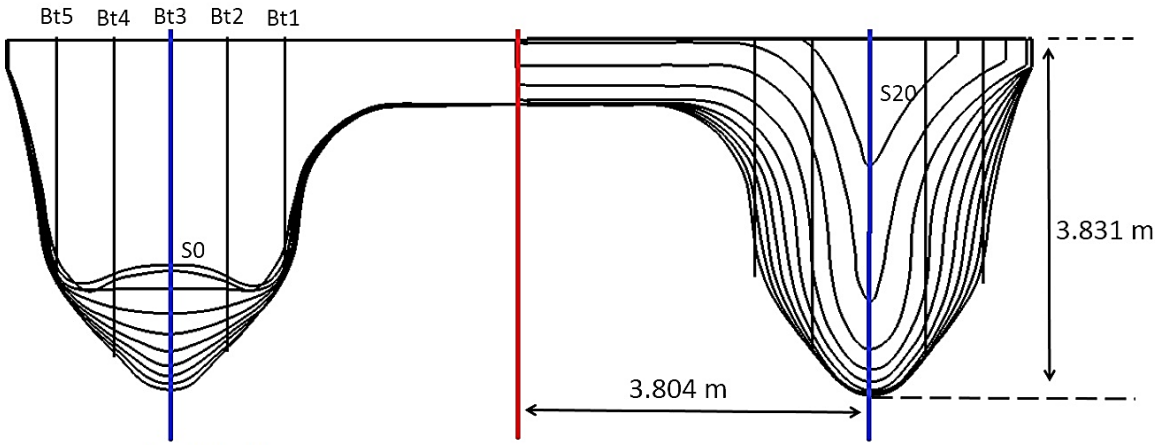

(b) Body lines

Figure 1: Geometry of AUT-SEM00 ship

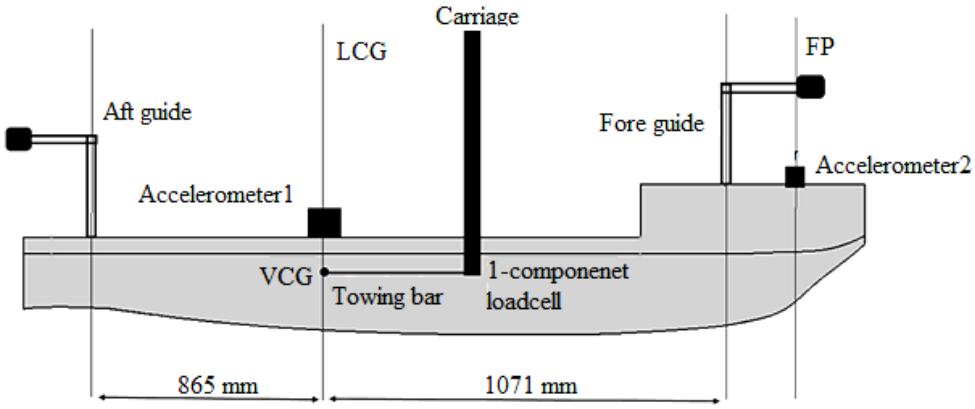

Figure 2: Model setup and measuring equipment

Figure 3: Measuring and setting up the moment of inertia of the model.

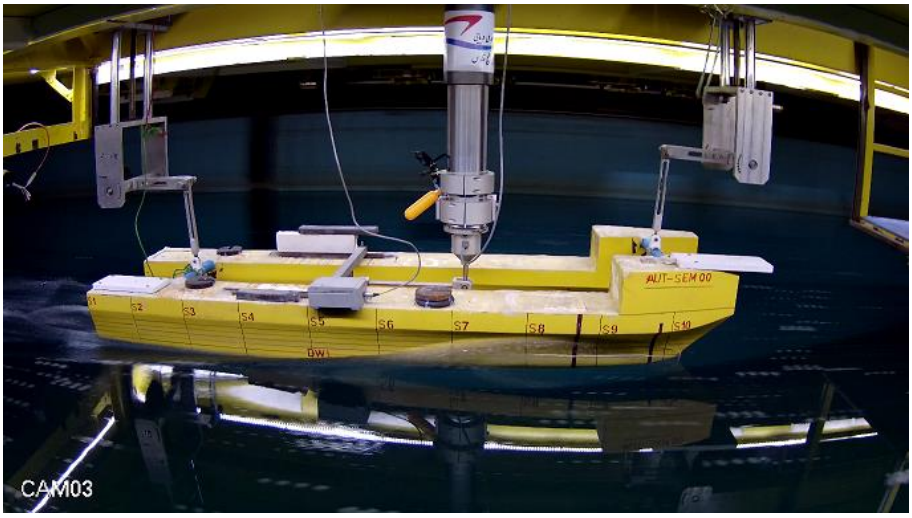

Figure 4: The resistance test at a speed of 4.41 m/s and 0.0º static trim angle

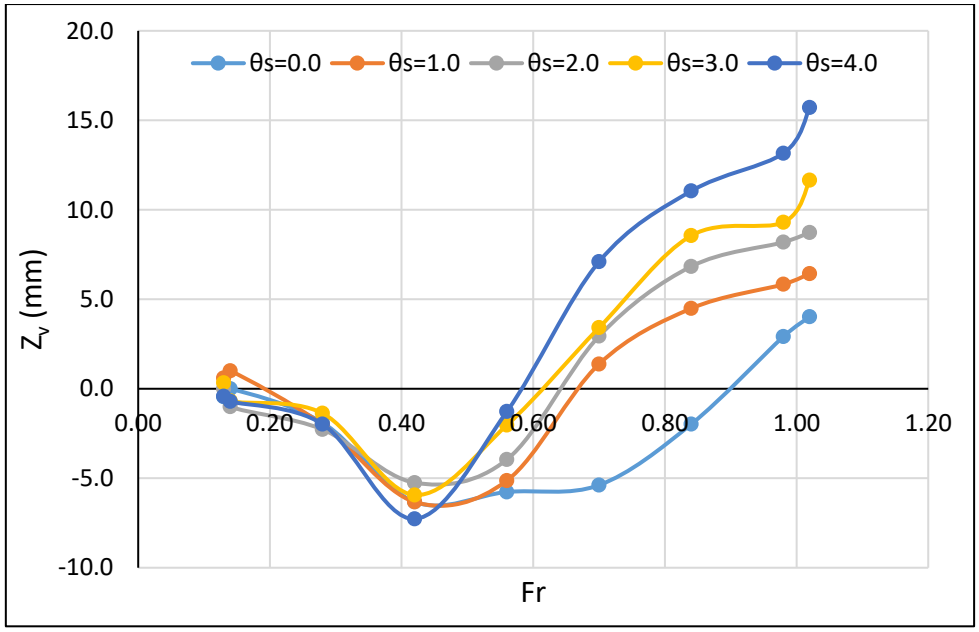

Figure 5: Rise-up versus Fr in a range of static trim angle

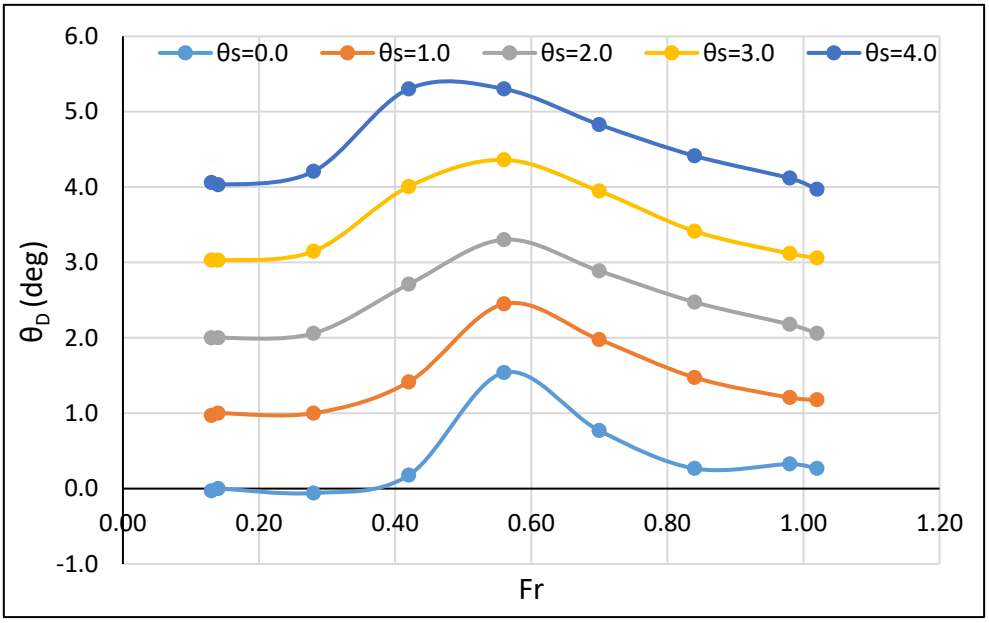

Figure 6: Dynamic trim versus Fr in a range of static trim angle

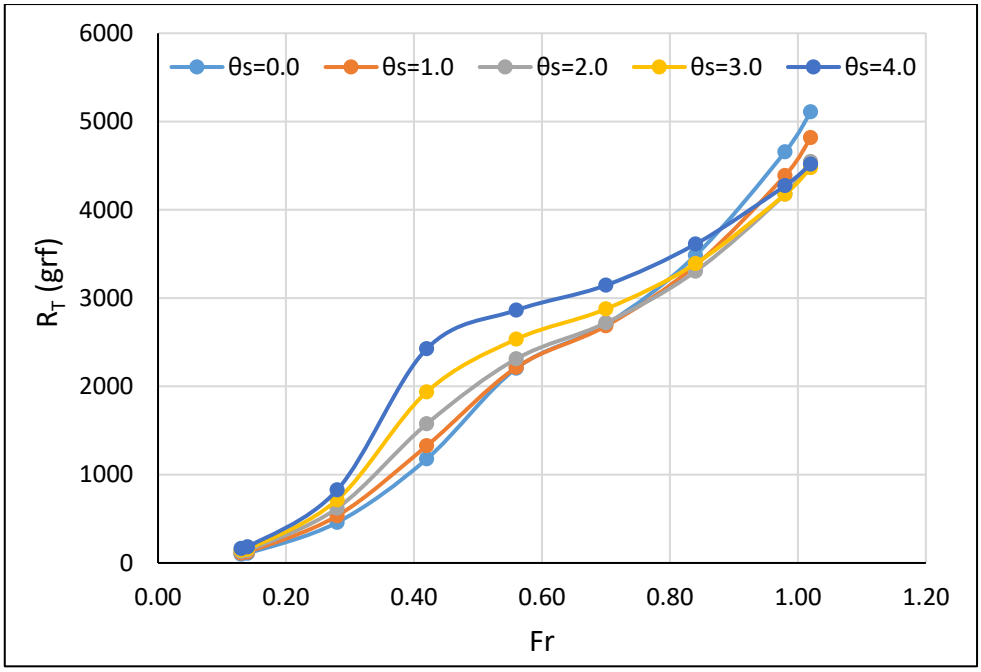

Figure 7: Resistance versus Fr in a range of static trim angle

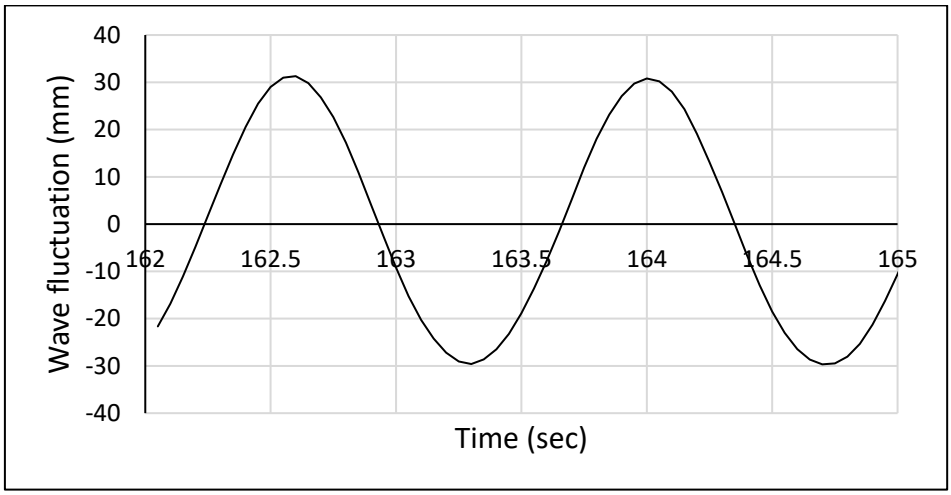

Figure 8: Time series of the wave profile at Run # 2.

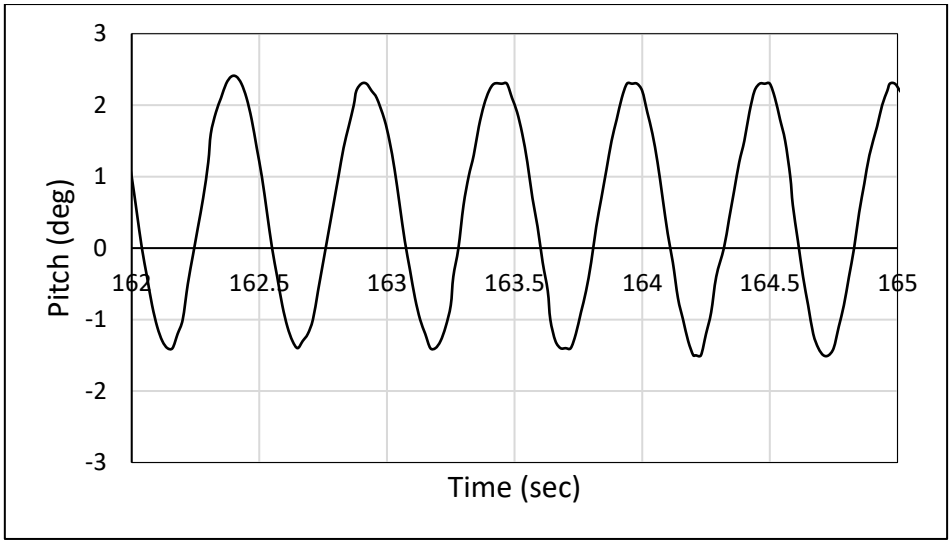

Figure 9: Time series of pitch motion at Run # 2.

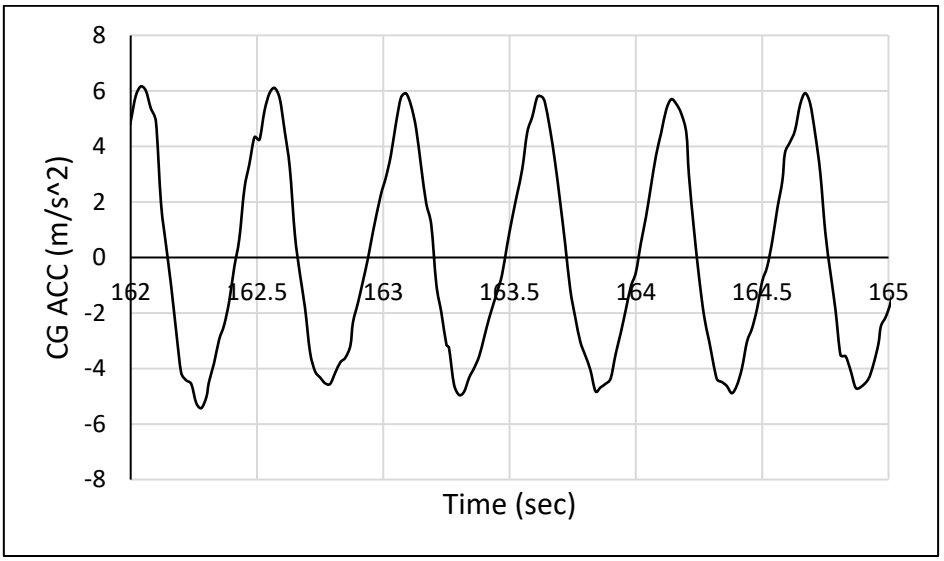

Figure 10: Time series of vertical acceleration of CG at Run # 2.

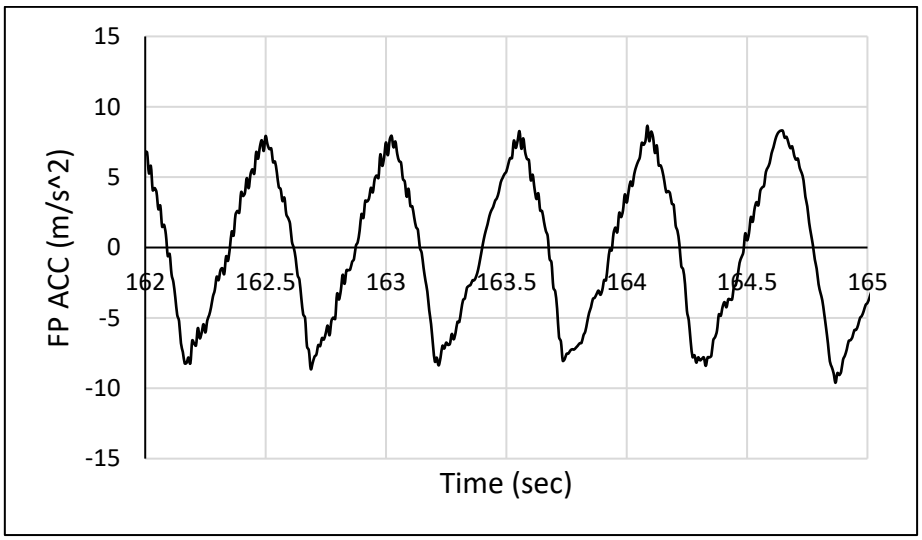

Figure 11: Time series of vertical acceleration of FP at Run # 2.

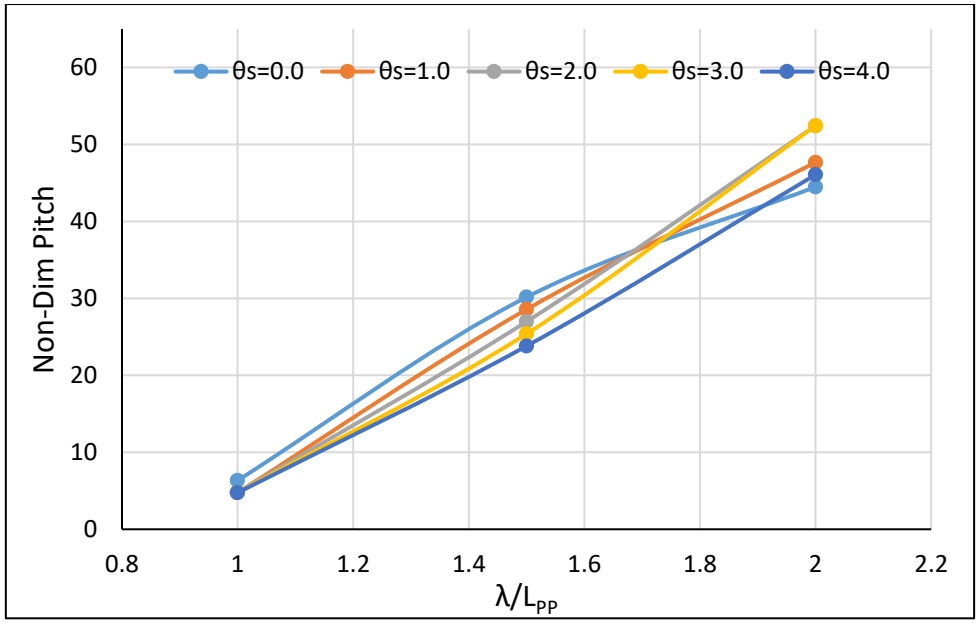

Figure 12: non-dimensional pitch versus λ/L_{PP} in a range of static trim angles.

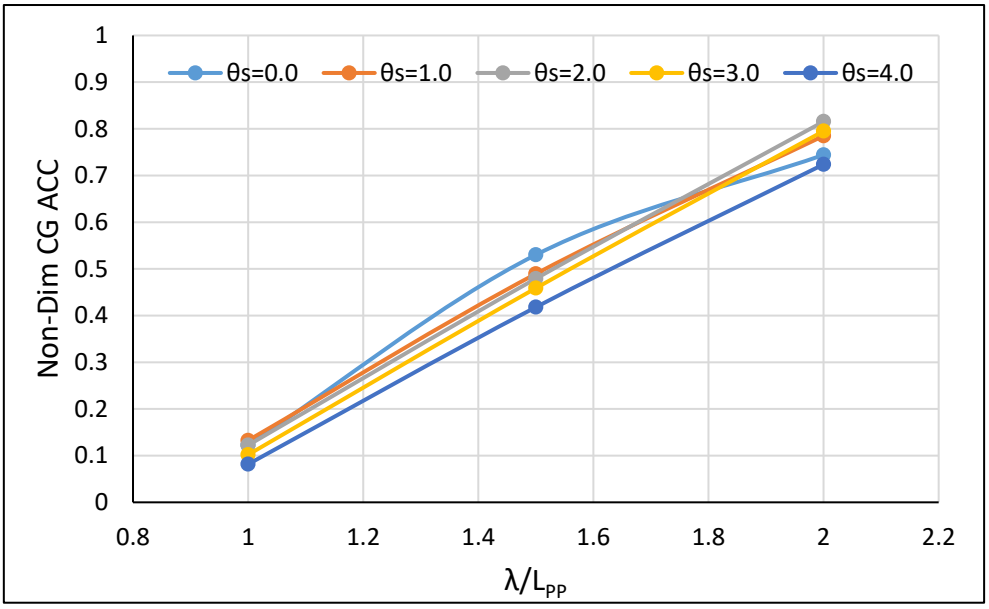

Figure 13: non-dimensional CG acceleration versus λ/L_{PP} in a range of static trim angles.

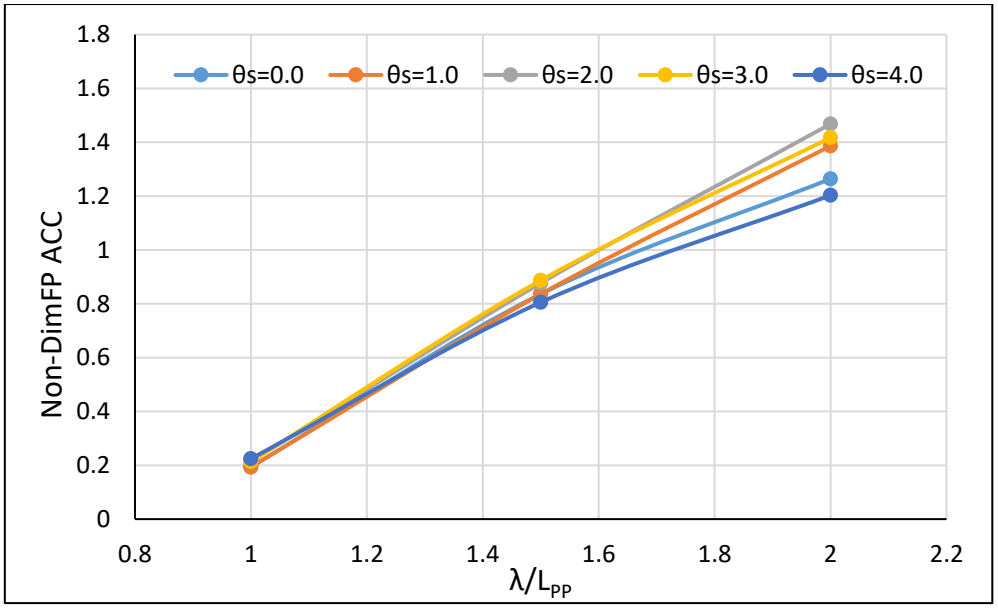

Figure 14: non-dimensional FP acceleration versus λ/L_{PP} in a range of static trim angles.

Tables

Table 1: Specifications of AUT-SEM00 ship and model

Parameter	Unit	Ship	Model
L_{OA}	m	37.50	2.250
L_{WL}	m	34.73	2.083
B_T	m	11.21	0.672
T	m	1.81	0.109
Δ	kg	161570	34.12
ρ	kg/m^3	1025	1002
λ	-	1:1	1:16.67
P_B	kW	3152	-
V	kn or m/s	30.0 (kn)	3.78 (m/s)

Table 2. Hydrostatic properties of the AUT SEM00 model in trim conditions at the displacement of 34.12 kg.

No.	L_{CG} (m)	θ_s (deg)	TF (m)	TA (m)
1	1.003	0.0	0.107	0.107
2	0.923	1.0	0.086	0.122
3	0.844	2.0	0.064	0.137
4	0.768	3.0	0.042	0.151
5	0.698	4.0	0.020	0.166

Table 3. NIMALA Towing Tank specifications

L (m)	402.0
b (m)	6.0
H (m)	4.5
h (m)	4.0
$\boldsymbol{Vc}$ (m/s)	19.00
Wave-maker Type	segmented plate-type
Max H_w (m)	0.50
Wave Recording System	wave probe, resistive

Table 4: Model test scenario of the calm water

Static trim angle (deg)	Fr	V_K (ship)	V (model)
From 0.0° to 4.0° at the step of 1.0°	0.13	4.75	0.60
	0.14	5.00	0.63
	0.28	10.00	1.26
	0.42	15.00	1.89
	0.56	20.00	2.52
	0.70	25.00	3.15
	0.84	30.00	3.78
	0.98	35.00	4.41
	1.02	36.75	4.63

Table 5: Model test scenario of motion in regular waves at a speed of 3.78 m/s

Run #	θ_s (deg)	H_w (m)	T (sec)	λ/L_{pp}
1	0.0	0.0418	1.16	1.00
2		0.0626	1.42	1.50
3		0.0834	1.63	2.00
4	1.0	0.0418	1.16	1.00
5		0.0626	1.42	1.50
6		0.0834	1.63	2.00
7	2.0	0.0418	1.16	1.00
8		0.0626	1.42	1.50
9		0.0834	1.63	2.00
10	3.0	0.0418	1.16	1.00
11		0.0626	1.42	1.50
12		0.0834	1.63	2.00
13	4.0	0.0418	1.16	1.00
14		0.0626	1.42	1.50
15		0.0834	1.63	2.00

Table 6: model test results in calm water in a range of static trim angles and speeds

θ_s (deg)	Fr	V (m/s)	R_T (grf)	Up (%)	Θ_D (deg)	Ut (%)	Z_v (mm)	Ur (%)
	0.13	0.60	98	0.2568	-0.0	1.02	-0.5	1.17
	0.14	0.63	108	0.2430	0.0	0.60	0.00	0.98
	0.28	1.26	459	0.3035	-0.1	0.49	-1.9	0.49
	0.42	1.89	1178	0.1898	0.2	0.30	-6.3	0.33
0.0	0.56	2.52	2205	0.1698	1.5	0.22	-5.8	0.77
	0.70	3.15	2701	0.1670	0.8	0.18	-5.4	0.07
	0.84	3.78	3484	0.1647	0.3	0.15	-2.0	0.04
	0.98	4.41	4656	0.1631	0.3	0.13	2.9	0.67
	1.02	4.63	5109	0.1628	0.3	0.14	4.0	0.90
	0.13	0.60	111	0.2399	1.0	1.08	0.6	1.26
	0.14	0.63	123	0.2277	1.0	0.65	1.0	1.03
	0.28	1.26	534	0.2735	1.0	0.52	-2.0	0.52
	0.42	1.89	1327	0.1841	1.4	0.33	-6.3	0.36
1.0	0.56	2.52	2215	0.1697	2.5	0.24	-5.1	0.82
	0.70	3.15	2685	0.1670	2.0	0.20	1.4	0.08
	0.84	3.78	3371	0.1649	1.5	0.17	4.5	0.04
	0.98	4.41	4389	0.1634	1.2	0.14	5.8	0.70
	1.02	4.63	4818	0.1630	1.2	0.15	6.4	0.99
	0.13	0.60	126	0.2245	2.0	1.19	0.0	1.33
	0.14	0.63	139	0.2149	2.0	0.71	-1.0	1.08
	0.28	1.26	620	0.2493	2.1	0.57	-2.3	0.57
	0.42	1.89	1575	0.1778	2.7	0.35	-5.3	0.39
2.0	0.56	2.52	2312	0.1691	3.3	0.26	-4.0	0.88
	0.70	3.15	2720	0.1669	2.9	0.21	2.9	0.08
	0.84	3.78	3303	0.1651	2.5	0.18	6.8	0.04
	0.98	4.41	4178	0.1636	2.2	0.15	8.2	0.75
	1.02	4.63	4546	0.1632	2.1	0.16	8.7	1.05
	0.13	0.60	144	0.2117	3.0	1.28	0.3	1.42
	0.14	0.63	154	0.2063	3.0	0.77	-0.7	1.13
	0.28	1.26	715	0.2306	3.2	0.62	-1.4	0.62
	0.42	1.89	1937	0.1723	4.0	0.37	-5.9	0.42
3.0	0.56	2.52	2535	0.1678	4.4	0.28	-2.0	0.97
	0.70	3.15	2877	0.1663	4.0	0.22	3.4	0.09
	0.84	3.78	3390	0.1649	3.4	0.19	8.6	0.05
	0.98	4.41	4175	0.1636	3.1	0.15	9.3	0.83
	1.02	4.63	4476	0.1633	3.1	0.17	11.7	1.14
	0.13	0.60	164	0.2015	4.1	1.38	-0.4	1.50
	0.14	0.63	182	0.1948	4.0	0.84	-0.7	1.25
	0.28	1.26	827	0.2153	4.2	0.65	-2.0	0.66
	0.42	1.89	2426	0.1684	5.3	0.40	-7.3	0.45
4.0	0.56	2.52	2863	0.1664	5.3	0.30	-1.3	1.04
	0.70	3.15	3145	0.1655	4.8	0.24	7.1	0.09
	0.84	3.78	3612	0.1644	4.4	0.21	11.1	0.05
	0.98	4.41	4273.1	0.1635	4.1	0.17	13.2	0.88
	1.02	4.63	4517	0.1632	4.0	0.19	15.7	1.24

Table 7: Model test results in waves in a range of static trim angles.

θ_s(deg)	Run No	η_θ (deg)	$\eta_{CG\ ACC}$ (m/s^2)	$\eta_{FP\ ACC}$ (m/s^2)
	1	0.4	1.2	1.9
0.0	2	1.9	5.2	8.2
	3	2.8	7.3	12.4
	1	0.3	1.3	1.9
1.0	2	1.8	4.8	8.2
	3	3.0	7.7	13.6
	1	0.3	1.2	2.1
2.0	2	1.7	4.7	8.6
	3	3.3	8.0	14.4
	1	0.3	1.0	2.1
3.0	2	1.6	4.5	8.7
	3	3.3	7.8	13.9
	1	0.3	0.8	2.2
4.0	2	1.5	4.1	7.9
	3	2.9	7.1	11.8